Impacts of surface roughness lengths on axisymmetrically mean structure of Typhoon Fanapi (2010)

Akiyoshi Wada
*Meteorological Research Institute, Tsukuba, Ibaraki, 305-0052, JAPAN
*awada@mri-jma.go.jp

1. Introduction

Ocean waves cause variation in surface roughness lengths over the ocean particularly during the passage of tropical cyclones (TC). Wada and Kohno (2012) investigated the impact of surface roughness lengths on TC simulations. They concluded that the impact on TC track simulations was negligibly small but that on simulated central pressure was ~10 hPa during the intensification of simulated Typhoon Fanapi in 2010. The exchange coefficient for the momentum flux associated with surface roughness lengths plays an important role in estimation of the effect of surface friction on inward angular momentum transport, because surface friction is considered to affect tangential winds and radial inflow and thereby secondary circulation. However, Wada and Kohno (2012) did not address impacts of surface roughness lengths on the axisymmetrical structure of the typhoon.

In order to understand the effect of surface roughness lengths on the axisymmetrical structure of simulated typhoon, this study performed numerical simulations for Typhoon Fanapi (2010) using a nonhydrostatic atmosphere model coupled with an ocean wave model and a multi-layer ocean model (Wada et al., 2010) with a similar experimental design to Wada and Kohno (2012). The surface roughness length calculated by the coupled model is determined by the following five methods, respectively; functions of wave-induced stress (Janssen, 1991), wave age (Smith, 1992), wave steepness (Taylor and Yelland, 2001), the assumption of Charnock constant (Charnock, 1955), and drag coefficients depending on 10-m wind speed (Kondo, 1975).

2. Experimental design

Five numerical simulations were performed for Fanapi by using the coupled model incorporating each surface roughness length scheme mentioned above (Table 1). The coupled model covered a 2000 km x 1800 km computational domain with a horizontal grid spacing of 2 km. The coupled model had 40 vertical levels with variable intervals from 40 m for the near-surface layer to 1180 m for the uppermost layer. The coupled model had maximum height approaching ~23 km. The integration time was 72 hours with a time step of 6 s in the atmosphere model.

Oceanic initial conditions were obtained from the oceanic reanalysis datasets with horizontal resolution of 0.1°, calculated by the Meteorological Research Institute multivariate ocean variational estimation (MOVE) system (Usui, et al., 2006).

In the present study, the parameterization of ice nucleation proposed by Murakami (1990) was used instead of that of Meyer et al. (1992). Figure 1 shows time series of best-track central pressure and five simulated central pressures for Fanapi. The results of simulated central pressures slightly differed from those of Wada and Kohno (2012).

Table 1 List of numerical simulations, surface roughness scheme used, and horizontal resolution of oceanic initial condition.

Experiment		Surface roughness scheme	Horizontal resolution of MOVE
CH	CH1	Charnock (1955)	0.1°
JA	JA1	Janssen (1991)	0.1°
KO	KO1	Kondo (1975)	0.1°
SM	SM1	Smith (1992)	0.1°
TY	TY1	Taylor and Yelland (2001)	0.1°

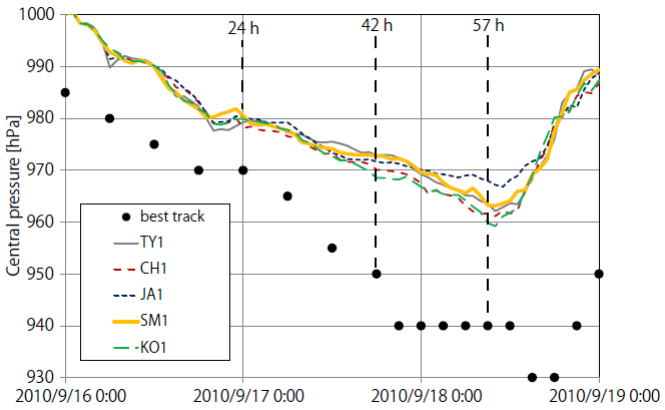

Figure 1 Time series of best-track central pressure and simulated ones.

3. Results

Figure 2 displays vertical profiles of axisymmetrically mean radial flow (contours) averaged among the five experiments with the standard deviations (shades) at 24 h (left panel), 42 h (middle panel) and 57 h (right panel). High standard deviations indicate that the impact of surface roughness lengths is high so that mean value is not significant. In other words, variation in surface roughness lengths is sensitive to axisymmetrically mean structure where the standard deviation is high. Figure 2 indicates that the inflow layer within the surface boundary layer is little affected by variation in surface roughness lengths, whereas outflows above the inflow layer and around 8000 m heights are sensitive to the variation. During the early intensification (24 h), axisymmetrically mean inflow layer relatively was thin and mean outflow above the mean inflow layer around the radius of 50 km was small. During the intensification phase (42 h), mean inflow reveals intrusion into the TC center. Axisymmetrically mean outflow above the mean inflow layer became high with high standard deviations around the radius of 50 km. During the mature phase (57 h), the mean inflow layer became thickest of the three integration times, indicating the occurrence of supergradient flow at the inner edge of mean inflow where high standard deviations appear. High standard deviations also appear along the inner side of the eyewall and around 8000 – 10000 m heights. These areas with high standard deviations correspond to the location of the secondary circulation.

Figure 3 displays vertical profiles of axisymmetrically mean equivalent potential temperature (contours) averaged among five experiments shown in Table 1 with the standard deviations (shades) at 24 h (left panel), 42 h (middle panel) and 57 h (right panel). During the early intensification (24 h), areas of higher mean equivalent potential temperature than the surrounding were relatively small around the TC center and the horizontal gradient was relatively small. During the intensification phase (42 h), the horizontal gradient became sharp around the radius of 50 -100 km and equivalent potential temperature became high. During the mature phase (57 h), the horizontal gradient became sharpest. The standard deviations of equivalent potential temperature were high above the inner edge of the inflow layer and around 8000 – 10000 m heights.

Figure 4 displays vertical profiles of axisymmetrically mean stability multiplying vertical velocity (contours) averaged among five experiments shown in Table 1 with the standard deviations (shades) at 24 h (left panel), 42 h (middle panel) and 57 h (right panel). Because high value of stability multiplying vertical velocity indicates high adiabatic cooling, Figure 4 reveals that adiabatic cooling within the eyewall is highly sensitive to variation in surface roughness lengths particularly during the mature phase (57 h). The sensitivity is also related to the process of the secondary circulation.

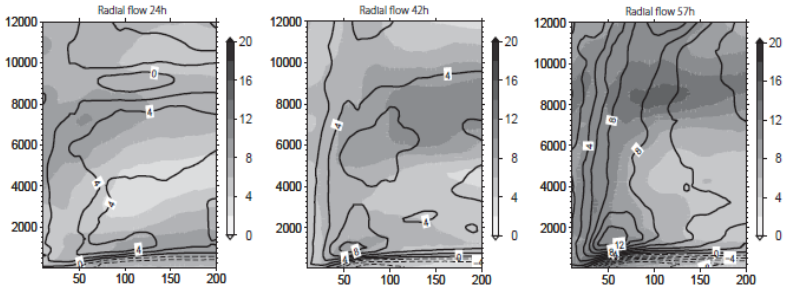

Figure 2 Vertical profiles of axisymmertically mean radial flow (contours) averaged among five experiments shown in Table 1 and the standard deviations (shades) at 24 h (left panel), 42 h (middle panel) and 57 h (right panel).

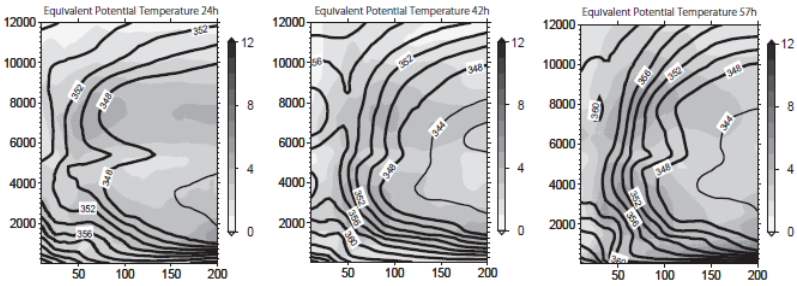

Figure 3 Same as Fig. 2 except for equivalent potential temperature.

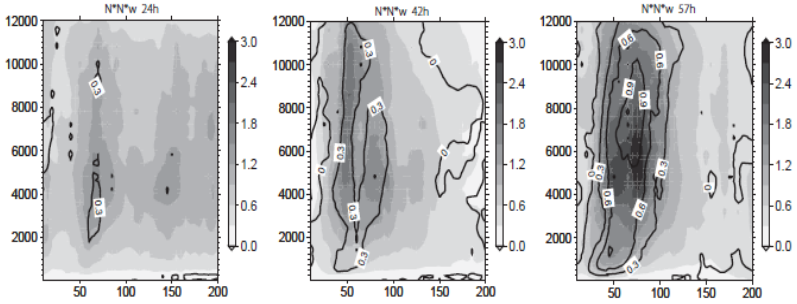

Figure 4 Same as Fig. 2 except for stability multiplying vertical velocity.

4. Discussion and conclusion

The impact of variation in surface roughness lengths on axisymmetrically mean structure of simulated Typhoon Fanapi (2010) appeared remarkably in the process of the secondary circulation at areas of supergradient inflow and associated outflow above the inner edge of the inflow layer, along the eyewall and around 8000 – 10000 m heights. It is noted that the impact on the inflow layer in the surface (frictional) boundary layer is relatively small although that on tangential flow is relatively high (not shown). The result may imply that the secondary circulation is not always forced by surface frictional inflow appeared in the surface boundary layer. We will further investigate the impact on the axisymmetrical structures of specific humidity and its horizontal flux in the future in order to understand the impact on microphysics associated with intensification process of simulated Fanapi.

Acknowledgements

This work was supported by the Japan Society for the Promotion of Science (JSPS), Grant-in-Aid for Scientific Research (C) (22540454) and on Innovative Areas (Research in a proposed research area) (23106505).

References

Charnock, H. (1955), Wind stress on a water surface, *Quart. J. Roy. Meteor. Soc.*, **81**, 639-640.

Jansen, P. A. E. M. (1991), Quasi-linear theory of wind-wave generation applied to wave forecasting, *J. Phys. Oceanogr.*, **21**, 1631-1642.

Kondo, J. (1975), Air-sea bulk transfer coefficients in diabatic conditions. *Bound. Layer Meteor.*, **9**, 91-112.

Louis, J. F., M. Tiedtke, and J. F. Geleyn (1982), A short history of the operational PBL parameterization at ECMWF. Proc. *Workshop on Planetary Boundary Layer Parameterization, Reading, United Kingdom*, ECMWF, 59–79.

Meyer, M. P., P. J. DeMott, and W. R. Cotton (1992), New primary ice-nucleation parameterizations in an explicit cloud model. *J. Appl. Meteor.*, 31, 708-721.

Murakami, M. (1990), Numerical modeling of dynamical and microphysical evolution of an isolated convective cloud – the 19 July 1981 CCOPE cloud. *J. Meteor. Soc. Japan*, 68, 107-128.

Smith, S. D., R. J. Anderson, W. A. Oost, C. Kraan, N. Maat, J. Decosmo, K. B. Katsaros, K. L. Davidson, K. Bumke, L. Hasse, and H. M. Chadwick (1992), The HEXOS results. *Boundary-Layer Meteorol.*, **60**, 109-142.

Taylor, P. K., and M. J. Yelland (2001), The dependence of sea surface roughness on the height and steepness of the waves. *J. Phys. Oceanogr.*, **31**, 572-590.

Usui, N., S. Ishizaki, Y. Fujii, H. Tsujino, T. Yasuda, and M. Kamachi (2006), Meteorological Research Institute multivariate ocean variational estimation (MOVE) system: Some early results. *Advances in Space Research*, **37**, 896-822.

Wada, A., N. Kohno and Y. Kawai (2010), Impact of wave-ocean interaction on Typhoon Hai-Tang in 2005, *SOLA*, **6A**, 13-16.

Wada, A. and N. Kohno (2012), Impact of surface roughness lengths on simulations of Typhoon Fanapi (2010), *CAS/JSC WGNE Res. Activ. Atmos. Oceanic. Modell.* **42**, 9-11